Published in final edited form as:
*Nat Cell Biol*. 2006 October ; 8(10): 1155–1162. doi:10.1038/ncb1477.

# The chaperonin TRiC controls polyglutamine aggregation and toxicity through subunit-specific interactions

**Stephen Tam**[1,2], **Ron Geller**[2], **Christoph Spiess**[2], and **Judith Frydman**[2,3]

[1] Biophysics Graduate Program, Stanford University, Stanford, California 94305, USA

[2] Department of Biological Sciences, Stanford University, Stanford, California 94305, USA

## Abstract

Misfolding and aggregation of proteins containing expanded polyglutamine repeats underlie Huntington's disease and other neurodegenerative disorders[1]. Here, we show that the hetero-oligomeric chaperonin TRiC (also known as CCT) physically interacts with polyglutamine-expanded variants of huntingtin (Htt) and effectively inhibits their aggregation. Depletion of TRiC enhances polyglutamine aggregation in yeast and mammalian cells. Conversely, overexpression of a single TRiC subunit, CCT1, is sufficient to remodel Htt-aggregate morphology *in vivo* and *in vitro*, and reduces Htt-induced toxicity in neuronal cells. Because TRiC acts during *de novo* protein biogenesis[2], this chaperonin may have an early role preventing Htt access to pathogenic conformations. Based on the specificity of the Htt–CCT1 interaction, the CCT1 substrate-binding domain may provide a versatile scaffold for therapeutic inhibitors of neurodegenerative disease.

Late-onset neurodegenerative diseases are often associated with the accumulation of insoluble amyloid aggregates in neurons[3]. In many cases, such as spinocerebellar ataxia and Huntington's disease, aggregation is associated with expanded polyglutamine (polyQ) tracts in the disease gene, usually beyond a critical threshold of approximately 40 glutamine repeats[1]. Because polyQ disease proteins are the main aggregate component in affected neurons[4], and glutamine tract length correlates with both aggregation propensity and age of onset of disease, it seems that toxic conformations of the polyQ-expanded proteins are directly responsible for neuronal dysfunction and death[1,5].

Recent studies suggest that the age-dependent accumulation of protein aggregates in neurodegenerative diseases reflects the progressive inability of the cellular quality control machinery to recognize and eliminate potentially toxic conformations. Molecular chaperones, which selectively bind non-native proteins and facilitate their folding or degradation[6,7], have been shown to modulate aggregation and toxicity in neurodegenerative disease models. In particular, overexpression studies have demonstrated that the chaperone Hsp70 and its cofactors, such as Hsp40, can remodel polyQ aggregates and alleviate the toxicity of polyQ aggregation[4]. Although these studies establish a role for chaperones in modulating polyQ aggregation, the chaperones that normally interact with pathogenic polyQ conformations and

3Correspondence should be addressed to J.F. (jfrydman@stanford.edu).

**AUTHOR CONTRIBUTIONS**

S.T. and J.F. planned the project. S.T., R.G. and C.S. prepared reagents and performed experiments. S.T., R.G., C.S. and J.F. designed experiments, interpreted data and wrote the manuscript.

**COMPETING FINANCIAL INTERESTS**

The authors declare that they have no competing financial interests.



Note: Supplementary Information is available on the Nature Cell Biology website.

prevent their aggregation *in vivo* have not been identified. Recently, a genome-wide RNAi screen in *Caenorhabditis elegans* searching for endogenous regulators of polyQ aggregation isolated, in addition to Hsp70 and Hsp40, six of the eight subunits of the eukaryotic chaperonin TRiC[8]. These findings raised the possibility that this chaperonin controls polyQ conformation *in vivo*. TRiC is an ATP-dependent ring-shaped hetero-oligomeric chaperone that binds and folds non-native polypeptides within its central cavity[9]. However, as TRiC folds essential cytoskeletal components, the observed RNAi phenotype could result from indirect effects on the cytoskeleton. Alternatively, because Hsp70 and TRiC cooperate in the *de novo* folding of several proteins[6,7,10], the screen may have uncovered the endogenous chaperone pathway for polyQ proteins.

The role of TRiC in polyQ aggregation was addressed using huntingtin (Htt), the causative agent of Huntington's disease. The naturally occurring amino-terminal proteolytic fragment (Htt-exon1) contains the highly polymorphic polyQ tract, and is sufficient for mediating Htt aggregation and cytotoxicity[4]. We exploited a well-established Htt aggregation model in *Saccharomyces cerevisiae* to determine whether TRiC functions in polyQ aggregation (Fig. 1). As reported, Htt-exon1 aggregates in a polyQ-length dependent manner and can be visualized by fusion to green fluorescent protein[11] (GFP; Fig. 1a, b). Whereas polyQ-expanded Htt-exon1 (Q103–GFP) aggregated into a single large inclusion body, the non-pathogenic Q25–GFP remained diffuse and soluble[11] (Fig. 1b, c). The extent of Q103–GFP aggregation was examined in cells with impaired TRiC function using the TRiC mutant strain *cct4-1*. Because all subunits are required for TRiC function, mutation or depletion of a single subunit is sufficient to impair the function of the complex[9]. Accordingly, *cct4-1* is defective in TRiC-mediated folding[10,12,13]. The number of cells containing large Q103–GFP aggregates increased by a factor of three when TRiC function was compromised (Fig. 1b, c). Importantly, expression of Q25–GFP in *cct4-1* cells did not result in increased aggregation, excluding the possibility that defects in TRiC function reduce the overall solubility of the GFP moiety (Fig. 1b, c). Increased polyQ aggregation in *cct4-1* cells was also observed using a biochemical assay that detects heat-stable, SDS-insoluble amyloid-like aggregates in cell extracts[5]. Whereas Q25–GFP formed only soluble species, Q103–GFP formed both soluble and heat-stable SDS-insoluble aggregates[11] (Fig. 1d). Consistent with our microscopy analysis, the amount of insoluble Q103–GFP was markedly increased in *cct4-1* cells (Fig. 1d).

The inhibitory role of TRiC on polyQ aggregation was further confirmed using two independent strategies. First, an increase in the number of cells containing Q103–GFP aggregates was observed in diploid cells heterozygous for *CCT4* (*CCT4/cct4Δ*) compared with wild type[14] (see Supplementary Information, Fig. S1a). In addition, direct depletion of CCT4 by transcriptional repression led to a significant increase in Q103–GFP aggregation (see Supplementary Information, Fig. S1b, c). We conclude that, as in *C. elegans*, TRiC is a key regulator of Htt aggregation in *S. cerevisiae*.

Second, we examined whether Htt physically interacts with TRiC. Purified GST–Htt-exon1 containing polyQ tracts of 18 (normal) or 51 (pathogenic) glutamines were incubated with yeast cell extract, and associated proteins were eluted and analysed (Fig. 2A). Interestingly, regardless of the polyQ length, Htt-exon1 interacts with TRiC and the yeast isoform of Hsp70 SSA (Fig. 2A). In contrast, no association was found with the abundant yeast isoform of Hsp70 SSB (Fig. 2A). Thus, Htt-exon1 interacts specifically with a subset of cytosolic chaperones. Furthermore, these interactions are not exclusive to the pathogenic variants of the protein.

The genetic and biochemical interactions described above suggest that TRiC interacts with and regulates polyQ conformations *in vivo.* We next examined whether TRiC suppresses Htt aggregation directly. To this end, a biochemical assay using purified components was used (Fig. 2). Soluble forms of normal (Q18) and pathogenic (Q51) Htt-exon1 were expressed and

purified as GST fusions (Fig. 2A). The unmodified Htt-exon1 variants were generated by TEV protease-mediated cleavage of the GST moiety. As shown previously, normal variants of Htt remain soluble, whereas pathogenic variants of Htt form heat-stable, SDS-insoluble aggregates that can be detected using a filter-trap assay[5]. Indeed, Q18 remained soluble, whereas Q51 formed large aggregates retained by the filter-trap (Fig. 2B, a). Importantly, addition of purified bovine TRiC directly suppressed aggregation of the purified pathogenic length Htt-exon1 in a concentration-dependent manner (Fig. 2B, b). TRiC was more effective than either Hsp70 or Hsp40 at the same molar ratios over Htt–polyQ (Fig. 2B, b; and data not shown). Formation of large fibrillar Htt aggregates is a nucleation-dependent process that involves several small oligomeric intermediates and has a lag phase of ~4–5 h[5]. To determine whether TRiC acts to prevent aggregate formation or to dissociate existing aggregates, we examined whether time-dependent addition of TRiC affected polyQ aggregation (Fig. 2C). Aggregation was initiated by TEV protease-mediated cleavage of the GST moiety and purified chaperone was added at different times during the lag phase. Both TRiC and Hsp70 prevented aggregate formation when added early during the lag phase, but did not dissociate preformed aggregates when added at 5 h (Fig. 2C). We conclude that TRiC directly inhibits Htt aggregation by binding early precursors of amyloid fibrils such as monomers and/or small oligomers.

The observation that TRiC is a potent inhibitor of polyQ aggregation led us to explore a strategy to increase TRiC activity *in vivo* and possibly prevent formation of pathogenic polyQ aggregates. The hetero-oligomeric TRiC chaperonin consists of eight unique subunits, CCT1–CCT8, which are thought to differ in their substrate binding specificities[9]. We hypothesized that Htt binding, and thus prevention of aggregation, may be mediated by specific interactions with selected subunits within the TRiC complex. To test this possibility, and thereby identify polyQ-interacting subunits, the effect of overexpressing individual TRiC subunits on polyQ aggregation was examined (Fig. 3a). Highly overexpressed TRiC subunits do not adversely affect cell viability (see Supplementary Information, Fig. S2 and data not shown). Moreover, native gel analysis and size exclusion chromatography indicated that overexpressing single chaperonin subunits did not affect the overall levels of the assembled TRiC complex (see Supplementary Information, Fig. S3a). The unincorporated overexpressed subunits remain soluble and elute as smaller molecular weight species (see Supplementary Information, Fig. S3b and data not shown). Strikingly, overexpression of selected TRiC subunits dramatically affected Htt aggregation (Fig. 3). Although the fraction of cells containing aggregates was unchanged, overexpression of subunits CCT1 and CCT4 had a dramatic effect on aggregate morphology (Fig. 3 and data not shown). Instead of the aggresome-like single large foci found on Q103–GFP induction, overexpression of CCT1 or CCT4 favoured the appearance of multiple, smaller foci reminiscent of those observed on overexpression of the Hsp70 SSA1 (Fig. 3b). In contrast, no change was observed by overexpression of the Hsp70 SSB2 (Fig. 3b, c)[15], consistent with the observation that SSB does not physically interact with Htt (Fig. 2a). The Htt structures induced by CCT1 and CCT4 possibly represent the SDS-soluble aggregates previously described for Hsp70 SSA1 overexpression[15–17].

Biochemical analysis of extracts overexpressing CCT1 showed that the fraction of the overexpressed subunit that was not assembled into the TRiC complex migrated as a monomeric species with a relative molecular mass ($M_r$) of 55,000 (see Supplementary Information, Fig. S3b). This suggests that the alteration of aggregate morphology observed when CCT1 is overexpressed is caused by free unassembled chaperonin subunits. Further supporting this hypothesis, CCT1 overexpression also remodelled aggregate morphology in *cct4-1* cells, without functional complementation of chaperonin function, indicating a direct action of the CCT1 subunit on Htt (see Supplementary Information, Fig. S4). Therefore, we hypothesized that these subunits may contain the Htt-exon1 binding determinants. To directly test this possibility, we used the *in vitro* aggregation assay with purified components described above (Fig. 2). Chaperonin subunits consist of three conserved domains: an ATP-binding equatorial

domain; a hinge-like intermediate domain; and an apical domain thought to contain the substrate binding sites (Fig. 3d). To investigate subunit-specific interactions with Htt-exon1, the apical domains of individual subunits were expressed and purified. The apical domain of CCT1 (ApiCCT1) was chosen as full-length CCT1 suppressed aggregation *in vivo* (Fig. 3c) and the apical domains of CCT3 and CCT7 served as controls (ApiCCT3 and 7, respectively). All three domains were correctly folded, as determined by circular dicroism spectroscopy (data not shown). Strikingly, purified ApiCCT1 suppressed polyQ aggregation in a concentration dependent manner, whereas the apical domains of subunits CCT3 and CCT7 did not inhibit aggregation (Fig. 3d). The observation that the apical domain of CCT1 is sufficient to prevent Htt aggregation independently of the entire chaperonin demonstrates that the TRiC subunits have evolved different substrate-binding specificities.

Although *S. cerevisiae* has proven to be an excellent and versatile model to understand the basic mechanisms of polyQ aggregation, mammalian cells are more physiologically relevant models to evaluate the links between Htt aggregation and toxicity. Thus, we tested whether RNAi-mediated downregulation of TRiC enhances aggregate formation in HeLa cells (Fig. 4). Short hairpin (sh)RNAs targeting TCP-β, the human homologue of CCT2, reduced TRiC levels by over 50–60% (Fig. 4a). Treatment with shRNA specific for TCP-β increased the number of cells containing large Q103–GFP aggregates by a factor of three over the shRNA control (Fig. 4b, c). In contrast, the solubility of Q25–GFP was not affected by TRiC depletion. These results indicate that TRiC is also a suppressor of polyQ aggregation in mammalian cells.

The role of TRiC in Htt aggregation and toxicity was further examined in a previously established neuronal cell model of Htt aggregation[18] — N2A cells stably expressing ponasterone A (PonA)-inducible Htt-exon1–Q150–GFP (Fig. 5). Fluorescence microscopy indicated that endogenous TRiC indeed associates with Htt aggregates upon induction of Q150–GFP (Fig. 5a). To assess the effect of CCT1 overexpression on aggregate morphology and toxicity, N2A cells stably expressing Htt-exon1–Qn–GFP ($n$ = 16, 150) were transfected with plasmids expressing yeast CCT1 or CCT7 subunits. In control cells, PonA induction of Q150–GFP led to formation of aggresome-like single large foci in ~25% of the cells (Fig. 5b and data not shown) and caused a marked increase in cell death (Fig. 5d). Although overexpression of CCT1 or CCT7 did not decrease the number of cells with aggregates, CCT1 favoured the appearance of many, smaller foci (Fig. 5b, c and data not shown). In contrast, overexpression of CCT7 did not change aggregate morphology. Remarkably, overexpression of CCT1, but not CCT7, protected cells from Htt-induced neurotoxicity (Fig. 5d). These results indicate that CCT1 overexpression in neurons can modulate aggregate morphology *in vivo* and suppress the formation of pathogenic conformations of Htt that lead to Huntington's disease-associated cell death.

The identification of TRiC as a key modulator of Htt aggregation and toxicity provides a unique insight into the physiological chaperone interactions of Htt. Unlike other chaperones linked to protein aggregation, the major cellular function of TRiC is to assist folding of newly translated polypeptides, rather than rescue stress-denatured proteins[19]. Therefore, the chaperonin is transcriptionally and functionally linked to protein synthesis and is not induced by stress[19]. Intriguingly, TRiC cooperates with Hsp70 during *de novo* folding of several proteins[2,10]. These observations, together with the finding that Htt interacts with both Hsp70 and TRiC, raise the possibility that the Hsp70–chaperonin pathway prevents aggregation by directing newly made Htt to non-pathogenic conformations (Fig. 5e). Consistent with this idea, we found that TRiC interacted with both normal and pathogenic forms of Htt (Fig. 2a). Our *in vitro* aggregation results further suggest that TRiC must act early in the lifespan of Htt to effectively modulate aggregation (Fig. 2c). Therefore, TRiC may determine the balance between toxic and non-toxic conformations of Htt (Fig. 5e). Further characterization of the chaperone-assisted folding pathway of Htt will be instrumental in understanding the genesis of Huntington's disease and

for the development of effective therapeutic approaches. As polyQ expansions are abnormal processes associated with a genetic defect, it is likely that the role of TRiC in determining the fate of Htt may illustrate a more general link between chaperones involved in *de novo* folding and the challenge of dealing with the continuous production of misfolded proteins.

Our findings that selected TRiC subunits suppress aggregation *in vitro* and toxicity *in vivo* support the hypothesis that individual subunits differ in their substrate specificity and suggest that Htt–TRiC interactions are mediated by contacts with yeast subunits CCT1 and CCT4. The effect of CCT1 and CCT4 overexpression on Htt–polyQ aggregates was similar to that observed by overexpression of the Hsp70 SSA1, suggesting that TRiC mediates neuroprotection by a mechanism similar to that described for Hsp70 (ref. [15]). Recent evidence suggests that the early soluble oligomeric intermediates in amyloid formation, rather than amyloid inclusion bodies themselves, are the cytotoxic species[17,20] (Fig. 5e). However, not all soluble aggregates are necessarily cytotoxic. *In vitro* studies defined a number of soluble polyQ oligomers, which include spherical, annular, protofibrillar and amorphous metastable structures[21]. Because Hsp70 attenuated formation of only the spherical and annular structures, it is possible that these oligomeric forms are the pathogenic agents[22]. Therefore, binding to Hsp70 or CCT1 may block formation of toxic amyloidogenic conformations and instead promote formation of non-toxic SDS-soluble aggregates.

An effective therapy for Huntington's disease remains elusive[23]. Our finding that the 140-amino-acid apical domain of CCT1 is a potent inhibitor of Htt–polyQ aggregation provides an intriguing avenue for therapeutic applications with several advantages over Hsp70-based approaches. First, the small CCT1 substrate-binding domain could provide a versatile scaffold for the design of polyQ aggregation inhibitors. Second, although Hsp70 and Hsp40 promiscuously chaperone a wide range of substrates and cellular interactions[6,7], TRiC, and in particular the CCT1 subunit, seem more restricted in their substrate binding range[9]. Therefore, CCT1-derived aggregation inhibitors could lead to specific therapeutics for the treatment of Huntington's disease and other neurodegenerative diseases.

## METHODS

### Yeast media and strains

Yeast strain genotypes are listed in the Supplementary Information, Table S1. Yeast media preparation, growth, transformations and manipulations were performed according to standard protocols[24]. The temperature-sensitive TRiC mutant allele *cct4-1* and the parental wild-type W303 strain were obtained from W. Zachariae (Max-Plank Institute of Molecular Cell Biology and Genetics, Dresden, Germany)[13]. *CCT4/cct4Δ* and CCT4/CCT4 strains RDY 56 and RDY 49, respectively, were obtained from R. Davis, (Stanford University, Stanford, CA)[14].

Haploid yeast containing one (wild-type) or no copies (*cct4Δ*) of CCT4, and covered by plasmid CCT4–HA–pESC, were constructed by tetrad dissection. Briefly, RDY 56 containing CCT4–HA–pESC was inoculated into 2 ml presporulation media (2% potassium acetate, 2% peptone, 1% yeast extract) overnight, washed twice with sterile water, resuspended in 2 ml sporulation media (1% potassium acetate, 1× URA dropout mix) and allowed to sporulate at room temperature for 5–7 days. Cells (50 μl) were washed and resuspended in sterile water, treated with 50 μl zymolyase (1 μg $\mu l^{-1}$) for 15 min at 37 °C, diluted with 300 μl sterile water and tetrad dissected on rich media plates containing galactose.

### Plasmids

Htt-exon1–GFP–pcDNA3.1 (Qn–GFP–pcDNA3.1; *n* = length of polyQ tract = 25 or 103; gift from R. Kopito, Stanford University, Stanford, CA)[25] was subcloned into galactose-inducible

pESC yeast expression vectors (Stratagene, La Jolla, CA). The GST–Htt-exon1 (GST–Qn, *n* = 18, 51; gift from R. Kopito, Stanford University, Stanford, CA) was previously described[25]. TRiC subunit CCTx (x = subunits 1–8) from yeast were HA-tagged and cloned into pESC, pCu426 and pcDNA3.1 expression vectors by PCR[27]. HA-tagged copper-inducible SSA1 and SSB2 constructs were kind gifts from V. Albanese (Stanford University, Stanford, CA). Qn–GFP–pCu constructs were made by replacing the galactose promoter from pESC with the CUP1 promoter (pCu). pSupCD4 was constructed by introducing truncated human CD4 lacking the cytoplasmic domain driven by a separate promoter into pSuperior vector (Oligoengine, Seattle, WA). The following primers were annealed, phosphorylated and cloned into pSupCD4 to generate pSupCD4–TCPβ: 5′-GATCCCCAGAAGACTGTGGAATCTGTTTCAAGAGAACAGATTCCACAGTCTTCTTTTTTA-3′ and 5′-AGCTTAAAAAAGAAGACTGTGGAATCTGTTCTCTTGAAACAGATTCCACAGTCTTCTGGG-3′.

## Antibodies

Anti-GFP antibodies were from Roche Diagnostics (Mannheim, Germany), anti-S-protein–HRP antibodies from EMD Biosciences (San Diego, CA), anti-HA antibodies from Sigma-Aldrich (St Louis, MO) and Alexa 594-conjugated secondary anti-rabbit antibodies from Molecular Probes (Eugene, OR). Other antibodies were previously described[19].

## Aggregation assays in yeast

Yeast containing the TRiC point mutant allele *cct4-1*, the parental wild-type allele (W303), one copy of CCT4 (*CCT4/cct4Δ;* RDY 56), or two copies of CCT4 (wild-type; RDY 49) were transformed with Qn–GFP–pESC (*n* = 25, 103) and grown overnight at 30 °C in liquid media containing 2% raffinose. Cells were diluted to $A_{600}$ = 0.2, allowed to grow for 1 h and induced with addition of 2% galactose. GFP-positive cells were scored for GFP foci at 24 h after galactose induction ($A_{600}$ <1.0).

Haploid yeast strains containing one (wild-type) or no copies (*cct4Δ*) of CCT4, covered by plasmid CCT4–HA–pESC, were transformed with Qn–GFP–pCu (*n* = 25, 103) and grown overnight at 30 °C in liquid media containing 2% galactose. Cells were harvested, washed once with sterile water, resuspended at 0 h in 200 μM $CuSO_4$-supplemented liquid media containing 2% glucose or 2% galactose to $A_{600}$ = 0.1 and allowed to grow for 24 h ($A_{600}$ <1.0). Cells were scored for GFP foci and aliquots were harvested at 0, 8 and 12 h. Cell pellets were lysed and analysed by SDS–PAGE as previously described[28].

The presence of insoluble aggregates in cells was assessed essentially as previously described[11]. Briefly, cells were lysed in an equivalent volume of stacker aggregation buffer (30 mM HEPES at pH 7.5, 150 mM NaCl, 5 mM $MgCl_2$, 10% glycerol, 0.5% NP-40) with an equivalent volume of glass beads, vortexed for 15 min at 4 °C, followed by centrifugation for 10 s at 14,000*g*. Equivalent total protein amounts from supernatants were run on SDS–PAGE and both stacking and resolving gels were transferred and analysed by immunoblot.

## *In vitro* GST–Qn aggregation assay

GST–Qn (*n* = 18, 51; 3 μM) was cleaved with TEV protease as described in TEV protocol (Invitrogen, Carlsbad, CA) in the presence of various chaperones or negative control ovalbumin (Sigma). All samples had equivalent amounts of chaperone buffer to normalize any effect of buffering conditions on TEV cleavage and Htt-exon1 aggregation. In addition, the chaperones did not affect the efficiency of TEV protease mediated cleavage (data not shown). At various times, reactions were stopped by the addition of an equivalent volume of 4% SDS, 100 mM DTT and boiled for 5 min as previously described[15]. Reactions were then filtered through 0.22

μm cellulose acetate (Schleicher & Schuell, Dassel, Germany), washed twice with 0.1% SDS, transferred to nitrocellulose for 10 min at 15 V, blocked in 2% milk (in TBS + 0.1% Tween) for 10 min and incubated with anti-S-protein–HRP blot for 1 h.

### Fluorescence microscopy

Yeast cells were washed once and resuspended in PBS, mounted onto coverslips and scored for GFP foci. Mammalian cells were split onto coverslips, washed twice with PBS, fixed with 4% paraformaldehyde (in PBS) for 20 min and washed twice with PBS. TRiC immunofluorescence microscopy was carried out after blocking in 2% BSA (in PBS), followed by anti-Tcpβ (rabbit) primary and Alexa 594-conjugated (anti-rabbit) secondary antibodies. Coverslips were mounted onto slide with fluoromount.

### GST pulldowns

Purified GST, GST–Q18 and GST–Q51 were prebound in equimolar amounts to glutathione–Sepharose beads (Amersham Biosciences, Piscataway, NJ) for 1 h at 4 °C, washed four times, resuspended 50:50 in PBS. This solution was mixed with 500 μg total protein lysate (W303) grown in YPD to $A_{600}$ = 0.9 and glass-bead lysed in Hsp90 buffer (10 mM Tris at pH 7.3, 50 mM NaCl, 50 mM KCl, 20 mM sodium molybdate, 10 mM $MgCl_2$, 20% glycerol) on a rotator for 1 h at 4 °C. Beads were washed four times with TBS plus 0.1% Tween and analysed by SDS–PAGE.

### Yeast TRiC subunit overexpression experiments

Wild-type (W303) yeast transformed with CCTx–HA–pESC (x = subunit 1–8) and Q103–GFP–pESC were grown overnight at 30 °C in liquid media containing raffinose. Cells were diluted to $A_{600}$ = 0.4, allowed to grow for 1 h and induced with addition of 2% galactose and 200 μM $CuSO_4$. GFP positive cells were scored for GFP foci at 24 h after galactose induction ($A_{600}$ <1.0).

Yeast native lysates were prepared by glass-bead lysis in native buffer (10 mM HEPES–HCl at pH 7.5, 50 mM Tris at pH 7.5, 100 mM KCl, 5 mM $MgCl_2$, 10% glycerol, 0.1% Triton and protease inhibitor cocktail) following lyticase treatment for 15 min at 30 °C. Native gels were run as previously described[10]. Size exclusion chromatography was carried out using Superose 6 or Superose 12 columns (Pharmacia, La Jolla, CA) equilibrated in native buffer according to the manufacturer's instructions.

### Mammalian cell culture

HeLa S3 cells were maintained in DMEM/F12 (Gibco, Carlsbad, CA), supplemented with 10% FCS and 3-glutamine. Confluent cells were transfected using Lipofectamine 2000 (Invitrogen) with pSupCD4–TCPβ (or vector alone) according to manufacturer's protocol. pSupCD4–TCPβ (or pSupCD4 alone) and Qn–GFP ($n$ = 25, 103) were cotransfected 24 h later. Cells were analysed 24 h later by microscopy or SDS–PAGE. Transient transfection of pSupCD4–TCPβ resulted in 60–70% transfection (as assessed by CD4 expression) and yielded a ~50–60% reduction of TRiC levels. As analysis of aggregation was carried out in CD4 expressing cells, the reduction of TRiC levels by shRNA is probably underestimated. Cells were lysed in lysis buffer (50 mM Tris–HCl at pH 8.8, 100 mM NaCl, 5 mM $MgCl_2$, 0.5% NP40, 1 mM EDTA) for 30 min on ice, followed by sonication.

Mouse neuro2a (N2A) cells stably transfected with Qn–GFP ($n$ = 16, 150) were a kind gift from N. Nukina (RIKEN Brain Science Institute, Wako City, Japan). They were maintained, differentiated and induced as previously described[18]. Confluent cells were transfected using Lipofectamine 2000 according to manufacturer's protocol and resulted in ~80% transfection.

Cells were differentiated and induced in dbcAMP (Sigma) and PonA (Invitrogen), respectively. Cell viability was assessed as described by 0.1% trypan blue staining (Sigma) using light microscopy[29].

### Protein purification

GST–Qn ($n$ = 0, 18, 51) were purified from BL21 cells with pROSETTA as previously described[5]. TRiC and Hsp70 was purified as previously described[2,30]. ApiCCTx–His (x = subunit 1, 3 or 7) were purified from BL21 cells with pROSETTA by Ni-NTA column.

## Supplementary Material

Refer to Web version on PubMed Central for supplementary material.

## Acknowledgments

We thank W. Zachariae, R. Kopito, R. Davis, N. Nukina and F. Sherman for kindly providing reagents and cells, P. Ren, V. Albanese, B. Riley, A.J. McClellan and other members of the Frydman and Kopito labs for advice and stimulating discussions and R. Andino for useful discussions and comments on the manuscript. This work was supported by National Institutes of Health (NIH) grants GM56433 and GM74074.

## References

1. Zoghbi HY, Orr HT. Glutamine repeats and neurodegeneration. Annu Rev Neurosci 2000;23:217–247. [PubMed: 10845064]
2. Frydman J, Nimmesgern E, Ohtsuka K, Hartl FU. Folding of nascent polypeptide chains in a high molecular mass assembly with molecular chaperones. Nature 1994;370:111–117. [PubMed: 8022479]
3. Soto C. Unfolding the role of protein misfolding in neurodegenerative diseases. Nature Rev Neurosci 2003;4:49–60. [PubMed: 12511861]
4. Muchowski PJ, Wacker JL. Modulation of neurodegeneration by molecular chaperones. Nature Rev Neurosci 2005;6:11–22. [PubMed: 15611723]
5. Scherzinger E, et al. Self-assembly of polyglutamine-containing huntingtin fragments into amyloid-like fibrils: implications for Huntington's disease pathology. Proc Natl Acad Sci USA 1999;96:4604–4609. [PubMed: 10200309]
6. Frydman J. Folding of newly translated proteins *in vivo*: the role of molecular chaperones. Annu Rev Biochem 2001;70:603–647. [PubMed: 11395418]
7. Hartl FU, Hayer-Hartl M. Molecular chaperones in the cytosol: from nascent chain to folded protein. Science 2002;295:1852–1858. [PubMed: 11884745]
8. Nollen EA, et al. Genome-wide RNA interference screen identifies previously undescribed regulators of polyglutamine aggregation. Proc Natl Acad Sci USA 2004;101:6403–6408. [PubMed: 15084750]
9. Spiess C, Meyer AS, Reissmann S, Frydman J. Mechanism of the eukaryotic chaperonin: protein folding in the chamber of secrets. Trends Cell Biol 2004;14:598–604. [PubMed: 15519848]
10. Melville MW, McClellan AJ, Meyer AS, Darveau A, Frydman J. The Hsp70 and TRiC/CCT chaperone systems cooperate *in vivo* to assemble the von Hippel-Lindau tumor suppressor complex. Mol Cell Biol 2003;23:3141–3151. [PubMed: 12697815]
11. Krobitsch S, Lindquist S. Aggregation of huntingtin in yeast varies with the length of the polyglutamine expansion and the expression of chaperone proteins. Proc Natl Acad Sci USA 2000;97:1589–1594. [PubMed: 10677504]
12. Vinh DB, Drubin DG. A yeast TCP-1-like protein is required for actin function *in vivo*. Proc Natl Acad Sci USA 1994;91:9116–9120. [PubMed: 7916461]
13. Camasses A, Bogdanova A, Shevchenko A, Zachariae W. The CCT chaperonin promotes activation of the anaphase-promoting complex through the generation of functional Cdc20. Mol Cell 2003;12:87–100. [PubMed: 12887895]
14. Deutschbauer AM, et al. Mechanisms of haploinsufficiency revealed by genome-wide profiling in yeast. Genetics 2005;169:1915–1925. [PubMed: 15716499]

15. Muchowski PJ, et al. Hsp70 and hsp40 chaperones can inhibit self-assembly of poly-glutamine proteins into amyloid-like fibrils. Proc Natl Acad Sci USA 2000;97:7841–7846. [PubMed: 10859365]

16. Muchowski PJ, Ning K, D'Souza-Schorey C, Fields S. Requirement of an intact microtubule cytoskeleton for aggregation and inclusion body formation by a mutant huntingtin fragment. Proc Natl Acad Sci USA 2002;99:727–732. [PubMed: 11792857]

17. Kayed R, et al. Common structure of soluble amyloid oligomers implies common mechanism of pathogenesis. Science 2003;300:486–489. [PubMed: 12702875]

18. Jana NR, Tanaka M, Wang G, Nukina N. Polyglutamine length-dependent interaction of Hsp40 and Hsp70 family chaperones with truncated N-terminal huntingtin: their role in suppression of aggregation and cellular toxicity. Hum Mol Genet 2000;9:2009–2018. [PubMed: 10942430]

19. Albanese V, Yam AY, Baughman J, Parnot C, Frydman J. Systems analyses reveal two chaperone networks with distinct functions in eukaryotic cells. Cell 2006;124:75–88. [PubMed: 16413483]

20. Arrasate M, Mitra S, Schweitzer ES, Segal MR, Finkbeiner S. Inclusion body formation reduces levels of mutant huntingtin and the risk of neuronal death. Nature 2004;431:805–810. [PubMed: 15483602]

21. Poirier MA, et al. Huntingtin spheroids and protofibrils as precursors in polyglutamine fibrilization. J Biol Chem 2002;277:41032–41037. [PubMed: 12171927]

22. Wacker JL, Zareie MH, Fong H, Sarikaya M, Muchowski PJ. Hsp70 and Hsp40 attenuate formation of spherical and annular polyglutamine oligomers by partitioning monomer. Nature Struct Mol Biol 2004;11:1215–1222. [PubMed: 15543156]

23. Marx J. Neurodegeneration. Huntington's research points to possible new therapies. Science 2005;310:43–45. [PubMed: 16210515]

24. Adams, A.; Gottschling, DE.; Daiser, CA.; Stearns, T. Methods in Yeast Genetics. Cold Spring Harbor Laboratory Press; New York: 1997.

25. Bence NF, Sampat RM, Kopito RR. Impairment of the ubiquitin-proteasome system by protein aggregation. Science 2001;292:1552–1555. [PubMed: 11375494]

26. Bennett EJ, Bence NF, Jayakumar R, Kopito RR. Global impairment of the ubiquitin–proteasome system by nuclear or cytoplasmic protein aggregates precedes inclusion body formation. Mol Cell 2005;17:351–365. [PubMed: 15694337]

27. Kabir MA, et al. Physiological effects of unassembled chaperonin Cct subunits in the yeast *Saccharomyces cerevisiae*. Yeast 2005;22:219–239. [PubMed: 15704212]

28. McClellan AJ, Scott MD, Frydman J. Folding and quality control of the VHL tumor suppressor proceed through distinct chaperone pathways. Cell 2005;121:739–748. [PubMed: 15935760]

29. Parran DK, Barker A, Ehrich M. Effects of thimerosal on NGF signal transduction and cell death in neuroblastoma cells. Toxicol Sci 2005;86:132–140. [PubMed: 15843506]

30. Ferreyra RG, Frydman J. Purification of the cytosolic chaperonin TRiC from bovine testis. Methods Mol Biol 2000;140:153–160. [PubMed: 11484484]

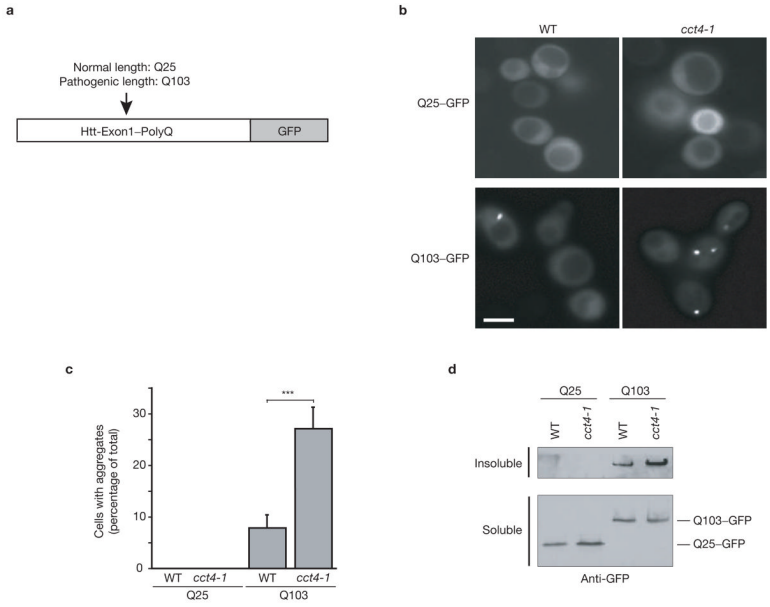


**Figure 1.**

Impaired TRiC function increases PolyQ-expanded huntingtin aggregation in budding yeast. (**a**) N-terminal Htt-exon1 fragment fused to C-terminal GFP (Htt-exon1–Qn–GFP: *n* = length of polyQ tract = 25 or 103) was used to monitor aggregation *in vivo*[11]. (**b**) Fluorescence microscopy of Htt-exon1–Qn–GFP (Qn–GFP) in wild-type (WT) or TRiC mutant (*cct4-1*) cells as described in methods[11]. The scale bar represents 5 μm. (**c**) Cells from **b** were scored for foci by visual inspection of GFP aggregates. Statistical analysis was performed using the one-sided, paired Student's *t*-test: mean ± s.e.m. of five independent experiments counting at least 200 cells each are shown (***$P < 0.001$). (**d**) Equivalent amounts of yeast cell lysates prepared from **b** were analysed for SDS-insoluble aggregates by anti-GFP immunoblot for high molecular weight species as previously described[11]. SDS-insoluble aggregates are retained in the stacking gel and SDS-soluble material enters the resolving gel. Representative results of at least three independent experiments are shown. See Supplementary Information, Fig. S5 for an uncropped image of the blot.

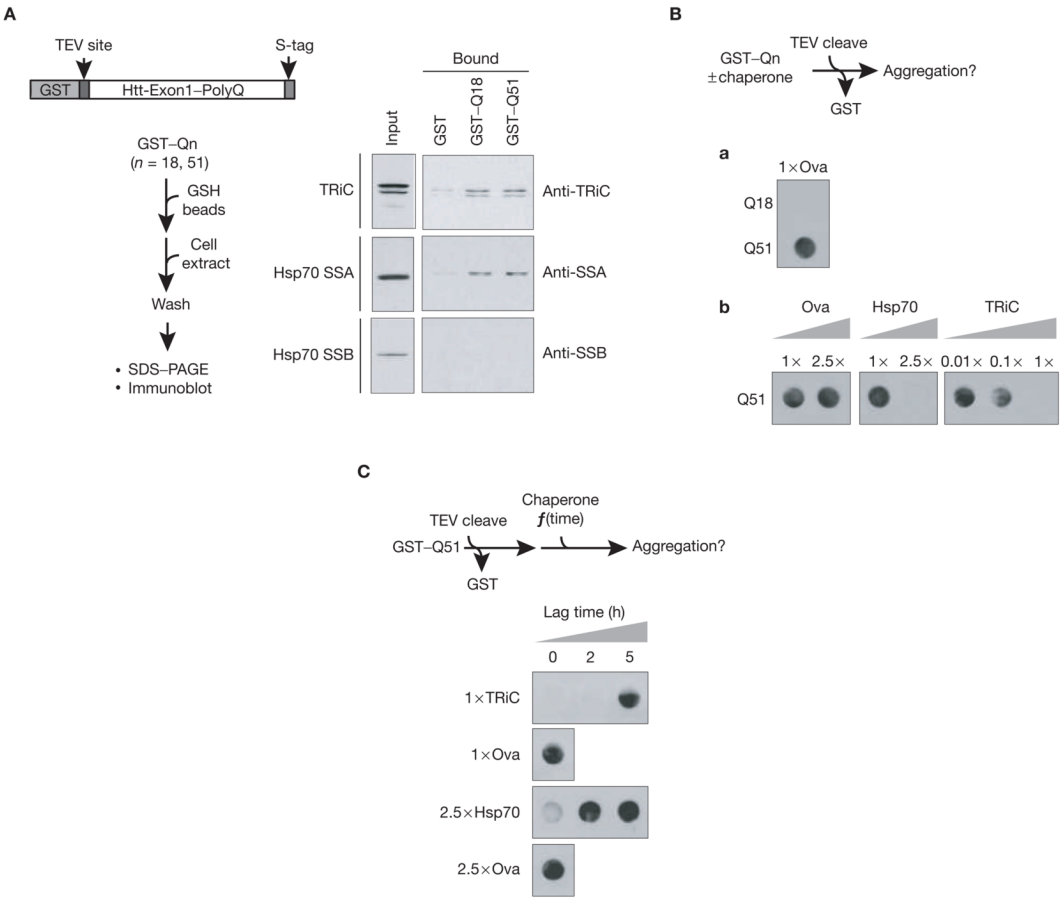


**Figure 2.**

TRiC physically interacts with and directly suppresses aggregation of PolyQ-expanded huntingtin. (**A**) All pulldown and *in vitro* aggregation assays were carried out as described in the methods[15] using Htt-exon1 carrying a C-terminal S-tag and an N-terminal GST moiety followed by a TEV protease cleavage site (GST–Qn). Isolation of cellular chaperones that interact with Htt was carried out by GST–Qn pulldown using glutathione–Sepharose (GSH) beads. Associated chaperones were detected by immunoblotting. Input was 5% total protein used in pulldown. See Supplementary Information, Fig. S5 for an uncropped image of the blot. (**B**) *In vitro* GST–Qn aggregation assay. SDS-insoluble, heat-stable aggregates were filter-trapped as described in the methods[15] and detected by anti-S-tag immunoblot. GST–Qn aggregation was assessed 6 h after TEV protease cleavage. Hsp70 served as a positive control and ovalbumin (Ova) as a non-specific negative control. Pathogenic length GST–Q51, but not normal length GST–Q18, forms SDS-insoluble, heat-stable aggregates (**a**). Chaperone-mediated suppression of GST–Q51 (**b**). Aggregation was assessed at indicated chaperone: GST–Q51 molar ratios. Chaperone addition did not inhibit TEV protease-mediated cleavage of GST–Q51 *in vitro* (data not shown). (**C**) Time course of chaperone addition. *In vitro* GST–Qn aggregation was initiated by TEV protease cleavage and indicated chaperone added at 0, 2, or 5 h post-TEV treatment. Reactions were stopped after 6 h and assayed as in **B**. Representative results of at least three independent experiments are shown.

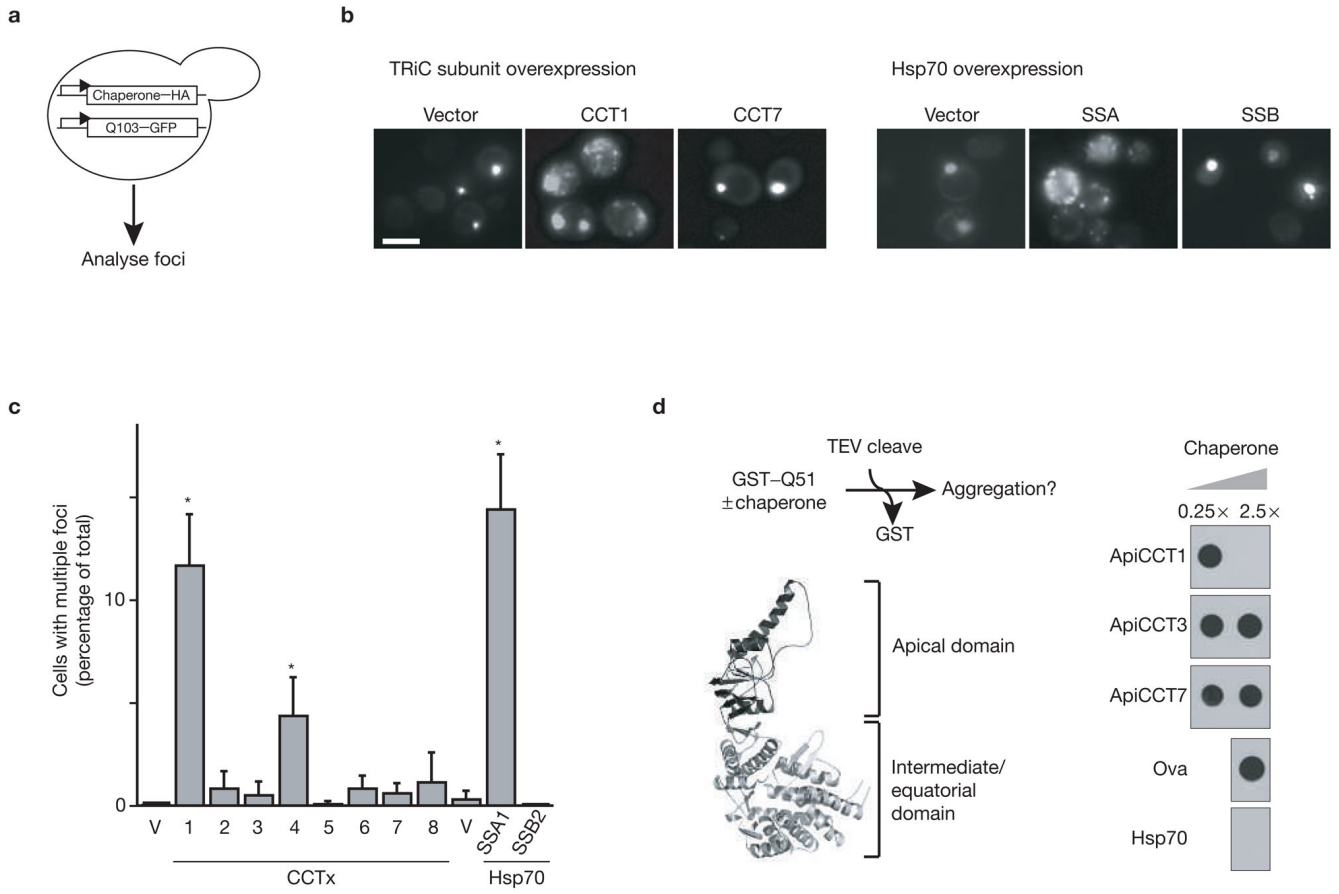


**Figure 3.**

Specific TRiC subunits directly modulate PolyQ-expanded huntingtin aggregate morphology. (**a**) Q103–GFP and chaperone–HA were co-overexpressed in wild-type (WT) cells for 24 h before analysis. (**b**) Fluorescence microscopy of Q103–GFP on coexpression of individual TRiC subunits (CCTx; x = subunits 1–8, shown for CCT1 and CCT7) and the yeast Hsp70s SSA1 and SSB2. The scale bar represents 5 μm. (**c**) Effect of chaperone overexpression on aggregate morphology. Distinct Q103–GFP aggregate morphologies, large single foci or multiple smaller diffuse aggregates, were assessed by visual inspection of GFP aggregates from **b**. Backbone vectors (V), were used as negative controls for TRiC subunits and SSA1, SSB2. Statistical analysis was performed using the one-sided, paired Student's *t*-test: mean ± s.e.m. of three independent experiments counting at least 200 cells each are shown (*$P$ <0.05). (**d**) Purified CCT1 apical domain specifically inhibits polyQ aggregation *in vitro*. A ribbon diagram of TRiC subunit domain architecture (modelled on an archaeal homologue, PBD accession number: 1A6E) is shown. Suppression of GST–Q51 aggregation by purified apical domains (ApiCCTx) corresponding to three TRiC subunits (CCT1, CCT3 and CCT7) was assessed at the indicated chaperone: GST–Q51 molar ratios as in Fig. 2b. Hsp70: positive control. Ova: non-specific protein control. Representative results of at least three independent experiments are shown.

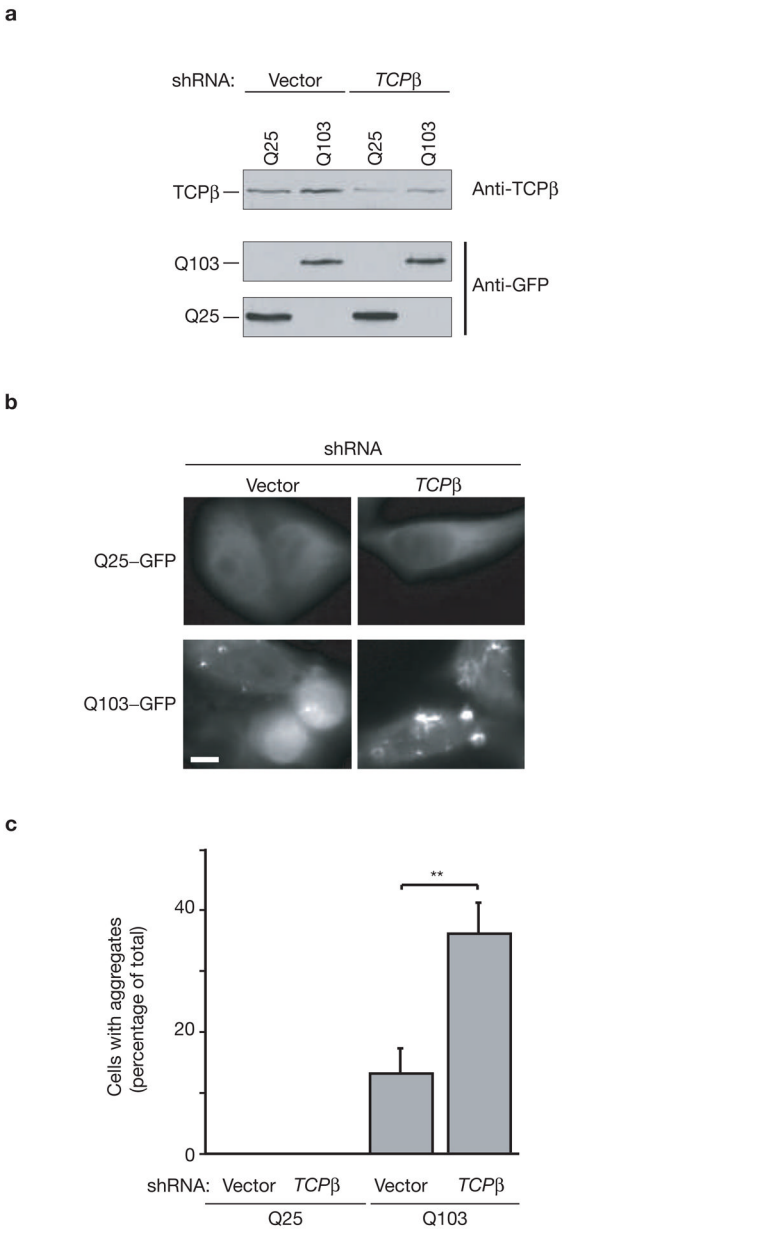


**Figure 4.**

Impaired TRiC function increases PolyQ-expanded huntingtin aggregation in mammalian cells. (**a**) Qn–GFP (*n* = 25, 103) and shRNA against TRiC subunit TCPβ were coexpressed by transient transfection in HeLa cells. TCPβ downregulation and Qn–GFP (*n* = 25, 103) expression were assessed by immunoblot analysis. TCPβ levels were reduced by at least 50–60% using shRNA targeting *TCPβ*, without affecting Qn–GFP expression levels. (**b**) Fluorescence microscopy of Qn–GFP (*n* = 25, 103) expressing HeLa cells from **a**. The scale bars represent 10 μm. (**c**) Cells from **b** were scored for foci by visual inspection of GFP aggregates. Statistical analysis was performed using the one-sided, paired Student's *t*-test: mean ± s.e.m. of three independent experiments counting at least 200 cells each are shown (**$P$ <0.01).

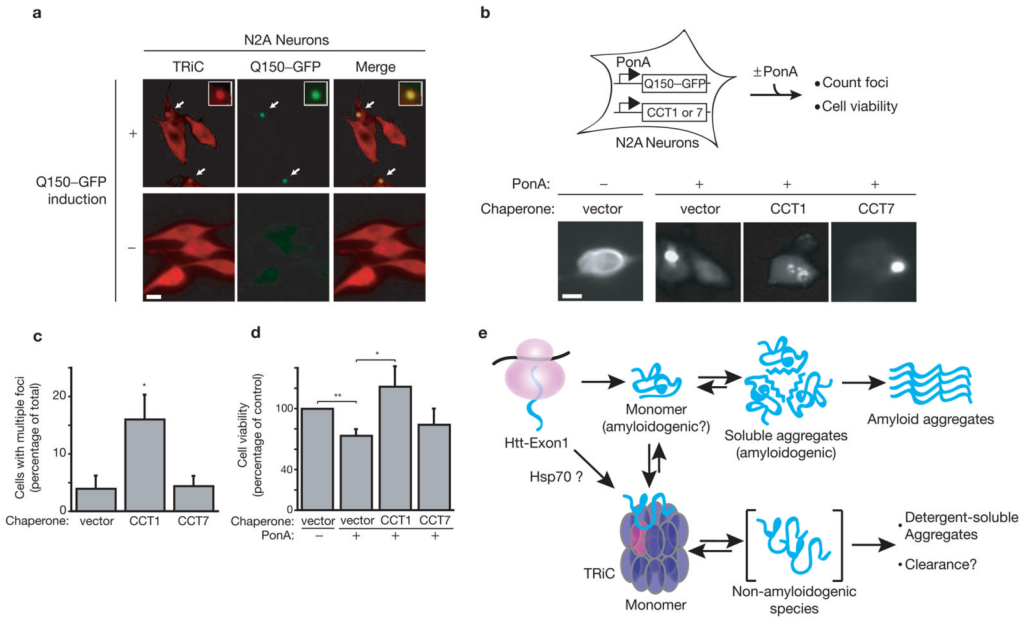


**Figure 5.**

TRiC modulates aggregation of PolyQ-expanded huntingtin and alleviates cytotoxicity in neurons. (**a**) TRiC colocalizes with PolyQ-expanded huntingtin in neurons. TRiC and Q150–GFP localization was detected by anti-TCPβ immunofluorescence and GFP fluorescence in Q150–GFP N2A neurons, respectively. The degree of colocalization was illustrated by merging TRiC and Q150–GFP images (merge). In control cells (−), Q150–GFP expression was not induced with PonA. Inset: larger image of a single aggregate highlights colocalization of TRiC with Htt aggregates in neurons. The scale bar represents 10 μm. (**b**) Fluorescence microscopy of Q150–GFP N2A neurons transiently transfected with CCT1, CCT7 or vector alone. In the control (−), Q150–GFP expression was not induced with PonA, but background Q150–GFP expression could still be detected. The scale bar represents 10 μm. (**c**) Q150–GFP aggregate morphology was assessed by visual inspection of GFP aggregates from **b**. Statistical analysis was performed using the one-sided, paired Student's *t*-test: mean ± s.e.m. of four independent experiments counting at least 200 cells each are shown. (**d**) Cell viability was assessed by trypan blue staining of neurons from **b** and normalized to uninduced control (−). Statistical analysis was performed using the one-sided, paired Student's *t*-test: mean ± s.e.m. of five independent experiments counting at least 200 cells each are shown (**P* <0.05; ***P* <0.01). (**e**) Role of the chaperonin TRiC in huntingtin biogenesis. Htt appears to interact with TRiC regardless of the polyQ length; the chaperonin partitions the Htt monomer away from the amyloidogenic pathway by promoting non-toxic conformations that can either be cleared and/or form detergent-soluble amorphous aggregates. This Htt–TRiC interaction is mediated by subunits CCT1–TCPβ and/or CCT4–TCPδ. The interaction seems to occur early in the aggregation pathway and may occur in cooperation with Hsp70.